

## Wavelet-based real-time ECG processing for a wearable monitoring system

Sebastian Zaunseder, Wolf-Joachim Fischer, Rüdiger Poll, Matthias Rabenau

### Angaben zur Veröffentlichung / Publication details:

Zaunseder, Sebastian, Wolf-Joachim Fischer, Rüdiger Poll, and Matthias Rabenau. 2008. "Wavelet-based real-time ECG processing for a wearable monitoring system." In *Proceedings of the First International Conference on Bio-inspired Systems and Signal Processing - Volume 2: BIOSIGNALS, (BIOSTEC 2008), January 28-31, 2008, Funchal, Madeira, Portugal*, edited by Pedro Encarnação and António Veloso, 255–60. Setúbal: SciTePress. <https://doi.org/10.5220/0001065002550260>.

# WAVELET-BASED REAL-TIME ECG PROCESSING FOR A WEARABLE MONITORING SYSTEM

S. Zaunseder and W.-J. Fischer

*Lifetronics, Fraunhofer Institute for Photonic Microsystems, Maria-Reiche-Strasse 2, 01109 Dresden, Germany  
sebastian.zaunseder@ipms.fraunhofer.de*

R. Poll and M. Rabenau

*Institute of Biomedical Engineering, Dresden University of Technology, Dresden, Germany  
Ruediger.Poll@tu-dresden.de*

**Keywords:** ECG processing, wavelet transform, shift-invariance, quadratic spline, real time, ambulatory monitoring, wearable, ultra-low power microcontroller, MIT-BIH Arrhythmia Database.

**Abstract:** This paper presents a wavelet-based signal processing method developed for an ambulatory ECG monitoring system. The monitoring system comprises modern trends in ambulatory ECG monitoring like integration of hardware in clothing, the use of low-power components and wireless data transmission via Bluetooth. The signal processing is located close to the sensor, thus allowing increased variability for the subsequent data handling (i.e. data transmission in case of detected abnormalities). Due to the very limited computational resources (an ultra-low power microcontroller ( $\mu C$ )) and the relatively high demands upon signal processing, the need arises for a method which meets the special demands of the ambulatory application. Therefore, we developed a wavelet-based method for detecting QRS complexes, especially adapted to the real-time requirements. The novel idea of our approach was to incorporate information gained from a lower scale directly into the threshold applied for QRS detection in a higher scale. To date, all tests proved a very low computational load while simultaneously preserving the reliability of the analysis (Se=99,74%, +P=99,85% using the entire MIT-BIH Arrhythmia Database), thus pointing out the possibilities of real-time signal processing under ultra-low power conditions.

## 1 INTRODUCTION

Analysis of the electrocardiogram (ECG) is used for diagnosis in a wide range of cardiac diseases. Anomalous changes may indicate arising coronary diseases in an early stage. Further on, acute life-threatening situations can be observed in the ECG immediately after their incidence. Increasingly powerful hardware today allows ambulatory long-time monitoring of the ECG. Such recordings are especially useful to detect sporadically occurring events, which are not perceptible in short-time readings. Also, the online observation of patients with increased risk of cardiac breakdowns, due to preliminarily diseases or due to special physiological stress, is feasible. The available possibilities make the long-time ECG a very powerful tool for improved medical care. The Fraunhofer Institute for Photonic Microsystems (IPMS) focuses on the development of a complete system for ambulatory

ECG monitoring. The signal processing is done in close proximity to the sensor to allow a high flexibility in further data handling. In particular, wireless data transmission can be reduced to situations of imminent risks, increasing the efficiency of the system to allow the long-time application (up to 7 days) of the system.

Due to the very limited resources of the employed ultra-low power  $\mu C$  and the often low signal quality, the demands on the signal processing are very high. The literature delivers a huge number of essays concerned with ECG processing: derivative based methods, digital filters, different transforms including the wavelet transform and neural networks, to name a few (Köhler, 2002). We designed a wavelet-based processing method especially suited for its real-time application. This paper describes the method and gives detailed information on the performance concerning detection rates as well as computational load.

The paper is organized as follows: Section 2 gives an introduction into the monitoring system and describes our algorithm based on considerations on the wavelet transform and its implementation in detail. Experimental results are reported in Section 3 and discussed in Section 4. Finally, Section 5 contains conclusions and some considerations concerning the future development of the system.

## 2 MATERIALS AND METHOD

### 2.1 Hardware

As carrier of the monitoring system we used a smart shirt. We integrated four electrodes to record a three-channel ECG based on Einthoven. Further on, a partially flexible printed circuit board was included. The board contains the hardware for analog preprocessing and further data handling. Sampling of the ECG is done at 1000 Hz and 12-Bit resolution. Data handling may include storage of data on a memory card and, optionally, the wireless data transmission via Bluetooth to a PDA. The PDA serves as gateway to communicate with medical personnel via internet. Signal processing done close to the sensor offers the possibility of wireless data transmission limited to situations of imminent risks. In this way, the actual data handling (storage and/or transmission) depends upon the outcome of the just-performed signal processing, thus rendering the overall system more flexible and improving its efficiency. All electronics as well as the signal processing is controlled by the ultra-low power  $\mu\text{C}$  MSP430F1611. Due to its low power consumption, such a controller is very suited for ambulatory applications. Of course, the low consumption accounts for a likewise low maximum clock frequency of 8 MHz. To handle this major drawback, an adequate signal processing method was developed. The underlying ideas, the implementation and performance results of the developed algorithm will be described next.

### 2.2 Signal Processing Method

#### 2.2.1 Wavelet Basics

The wavelet transform (WT) decomposes a signal in scaled and translated versions  $\psi_{a,t}(\tau)$  of a basis function called mother wavelet  $\psi(\tau)$ . The derivatives of the mother wavelet are given by

$$\psi_{a,t}(\tau) = \frac{1}{\sqrt{|a|}} \psi\left(\frac{\tau-t}{a}\right) \quad \text{with } a \in \mathbf{R}^+, t \in \mathbf{R} \quad (1)$$

where  $a$  is a scale factor which is a measure of the current width of the applied wavelet and  $t$  is the translation parameter which describes the position of the wavelet in the time domain. The wavelet transform  $X(a,t)$  results from the inner product of the signal and the scaled and translated wavelet

$$X(a,t) = \langle x, \psi_{a,t} \rangle = \int_{-\infty}^{+\infty} x(\tau) \frac{1}{\sqrt{|a|}} \psi^*\left(\frac{\tau-t}{a}\right) d\tau \quad (2)$$

The resulting coefficients can be seen as a measure for the similarity of the examined signal segment specified by  $t$ , and a wavelet of varying width specified by  $a$ . The transformation of (2) to the frequency domain yields

$$X(a,t) = \frac{\sqrt{|a|}}{2\pi} \int_{-\infty}^{+\infty} X(\omega) \Psi^*(\omega) e^{j\omega t} d\omega \quad (3)$$

where  $X(\omega)$  and  $\Psi(\omega)$  are the Fourier transforms of the signal and the wavelet, respectively. From (3) it can be seen that decomposing a signal by the WT is equivalent to the application of a filter bank. The bandwidth of each pass-band filter increases with higher center frequencies.

#### 2.2.2 Calculated Transform

There are three usual ways to compute the wavelet transform: the so-called continuous WT (CWT), the dyadic WT ( $D_Y\text{WT}$ ) and the discrete WT (DWT). The schemes differ in the required computational resources, the resulting degree of redundancy and in some properties of the results like shift-invariance. In the  $D_Y\text{WT}$  the scale  $a$  is sampled along a dyadic sampled grid while the translation remains scale independent. Thus, applying the  $D_Y\text{WT}$ , the property of shift-invariance can be maintained while the degree of redundancy, and therefore the computational load, is reduced in comparison to the CWT. For the  $D_Y\text{WT}$  the definition of  $\psi_{a,t}(\tau)$  becomes

$$\psi_{2^m,t}(\tau) = \frac{1}{\sqrt{2^m}} \psi\left(\frac{\tau-t}{2^m}\right) \quad \text{with } m \in \mathbf{Z}^+, t \in \mathbf{R} \quad (4)$$

When using expressions like “scale 4”, we will refer to the scale  $a=2^m=2^2$ .

Fast computations of the DWT are done through the Mallat algorithm. In analogy to the “algorithm à trous” (Holschneider, 1989), it constitutes a recursive algorithm allowing the fast calculation of

the  $D_YWT$ . The highly advantageous property of shift invariance justifies an increased computational effort, rendering the use of the  $D_YWT$  optimal for our intended realization.

A wide range of different wavelets have been employed in the past for ECG processing. Referring to the choice of an adequate wavelet, the statements found in the literature disagree. For instance, Dinh et al. conclude that the cubic spline wavelet is best suited for the detection of QRS complexes (Dinh, 2001). Differing from this, Li et al. do not perceive substantial differences in the performance of the detection by using a spline of higher order than the quadratic spline wavelet (Li, 1995). The possible usage of different wavelets allows the utilization of other criterions searching for an adequate one. As our application aims at the real-time processing under extremely limited resources, the compactness of the chosen wavelet in the time domain is a crucial demand. The quadratic spline wavelet originally introduced by Mallat et al. (Mallat, 1992) meets this demand and is used in our implementation. In Figure 1, the transfer functions realized by the quadratic spline wavelet are shown.

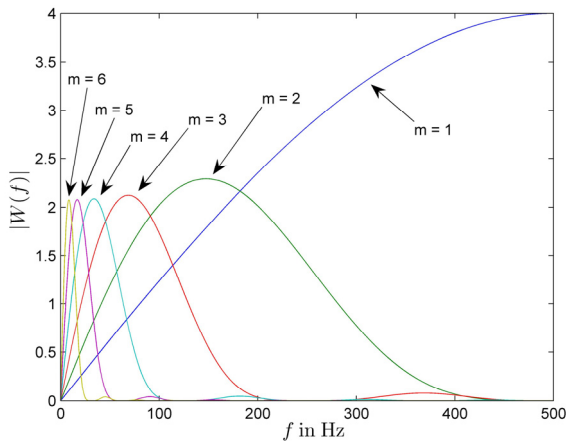


Figure 1: Transfer functions realized by the quadratic spline wavelet and a sampling frequency of 1000 Hz.

### 2.2.3 Underlying Idea of the Implemented Method

In the current stage of development we realized a QRS detector. The most commonly used principle of wavelet-based QRS detectors (employing the quadratic spline wavelet) is to search for modulus maximum pairs (MMP) (combination of local extreme values exceeding a threshold). To obtain a good performance the search typically is carried out across all scales, at least up to the scale assumed as most significant in regard to the main energy

portions contained in QRS complexes. (Li, 1995), (Martinez, 2004)

An obviously possible solution to reduce the computational effort is not to incorporate all scales, but to do the detection based on only one scale. Such an approach does not take advantage of the multi-scale decomposition provided by the WT, but it constitutes a viable way to detect QRS complexes. Employing only one scale of the WT is similar to the usage of a single bandpass-filter. On the filtered signal the typical method of grouping extrema to MMP and assigning them to QRS complexes can be applied. In Section 3, some example results (*testing1* and *testing2*, see Table 1) using this methodology are given. Different rules to control the value of the thresholds were employed. In both cases, adaptive thresholds (see Appendix for details on the adaptation) were applied. In *testing2* the threshold is generally endowed with an offset to lower the resulting value compared to the threshold in *testing1*. As expected, the performance of the methods varies in sensitivity and positive predictivity. Both methods offer, depending on the data set as well as on the observed signal portion within one data set, sections of varying detection quality. With regard to this, a method to influence automatically the valid threshold becomes a very interesting option. Such a procedure aims to take the advantages of a generalized lower or higher threshold according to the current signal state.

Our method detects QRS complexes in scale 5. Based on the number of threshold crossings within a sliding window in the scale 4 the threshold in scale 5 is controlled.

### 2.2.4 Structure of the Algorithm

The algorithm can be divided in three steps:

- (1) Search for MMP and extract “relevant threshold crossings” in scale 4.
- (2) Search for MMP in the scale 5 incorporating the information gained from the corresponding number of threshold crossings detected in the scale 4.
- (3) Classification of MMP found in scale 5 as QRS complexes using a simplified regularity analysis

Step (1): With every incoming sample the search for local extrema, aimed at the grouping of a MMP, is continued. Different combinations of extrema can constitute a MMP. To detect the extrema, online-adaptive thresholds  $\varepsilon_4^\pm$  are used. An adaptation of the thresholds is caused by the successful grouping of a MMP (see Appendix for details on the

adaptation). Based on  $\varepsilon_4^\pm$  additional thresholds  $\varepsilon_{cross}^\pm$  are created to excerpt all “relevant threshold crossings”. “Relevant threshold crossings” refer to local extrema crossing the corresponding threshold  $\varepsilon_{cross}^\pm$ . This registration is not carried out in order to group the extrema as MMP, but to obtain a measure of the signal quality by counting the number of crossings  $N_{cross}$  within a window  $W_{cross}$  of 500 samples. Note that there is a major difference between the extrema searched for MMP grouping and the extrema detected using  $\varepsilon_{cross}^\pm$ , as the absolute value of  $\varepsilon_{cross}^\pm$  is generally smaller or equal than  $\varepsilon_4^\pm$  and found extrema are not discarded until their position has left the range of the sliding window.

Step (2): MMP are searched in scale 5 using the same routine as in scale 4. Also online adaptive thresholds  $\varepsilon_5^\pm$  are existent. Differing from scale 4, for the MMP search in scale 5 not directly the online adaptive thresholds  $\varepsilon_5^\pm$  are used, but a threshold changed by a correction factor  $\kappa$ .  $\kappa$  varies depending on the number of registered threshold crossings. The actual number of zero crossings  $N_{cross}$  can be interpreted as a measure for the degree of higher frequency noise or artifacts. According to this,  $\kappa$  converts the information contained in  $N_{cross}$  to a threshold operation in scale 5, referred as  $\varepsilon_5^\pm + \kappa$  (note that this is only a symbolic notation). In general, for noisy segments the threshold is increased whereas a reduction in sections of good signal quality is performed. Depending on the value of  $N_{cross}$ , the modification of threshold can be up to  $\pm 37.5\%$  of the actual  $\varepsilon_5^\pm$ . It is important that the threshold be changed only for the search of local extrema, otherwise  $\varepsilon_5^\pm$  doesn't suffer any changes. To allow the zero crossing window to be placed symmetrically around the scale 5 coefficient under observation, the scale 5 coefficients have to be delayed by 250 samples (taking into account the half window size), plus the delay introduced by the recursive online calculation of the WT.

Step (3): If a MMP is detected in scale 5 and a corresponding MMP in scale 4 is existent, a simplified regularity analysis based only on the amplitudes of the detected MMP is carried out. If no corresponding MMP is present at scale 4, the MMP of scale 5 is accepted as QRS without any regularity analysis.

Figure 2 shows an example containing an ECG segment, the corresponding scale 4 and scale 5 coefficients and the course of. Also showed is the course of the threshold values  $\varepsilon_4^\pm$  (bright),  $\varepsilon_{cross}^\pm$  (dark),  $\varepsilon_5^\pm$  (bright),  $\varepsilon_5^\pm + \kappa$  (dark). The threshold adaptation after detections and the general dynamics of the correction factor are visible.  $N_{cross}$  exhibits the

expected behaviour. An increase is visible during noisy segments whereas during uncorrupted segments only the QRS complexes have an influence (resulting in an oscillation between 0 and 2 detected crossings).  $\varepsilon_5^\pm + \kappa$  oscillates around  $\varepsilon_5^\pm$ .

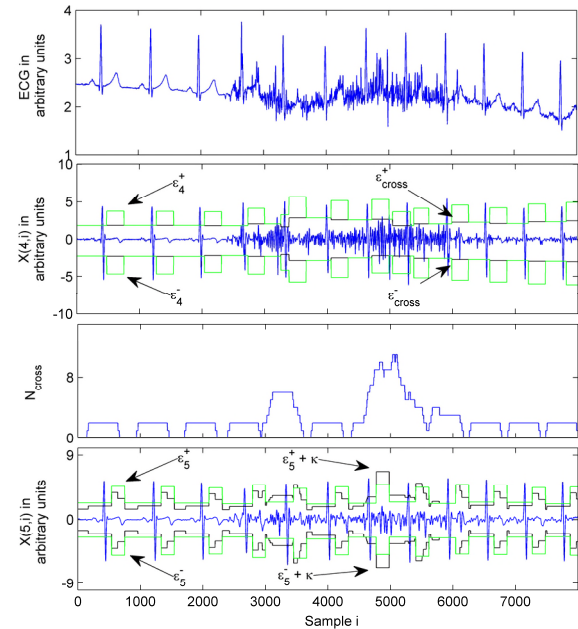


Figure 2: Example for the behavior of the algorithm.

## 2.2.5 Implementation

The algorithm was implemented in C. To minimize the required computational effort three fundamental concepts were incorporated in our implementation.

Simplicity of employed data types: the applied  $\mu C$  is a 16-Bit controller. This renders the application of 16 Bit fix-point operators very useful. Incoming data is sampled with a 12-bit resolution. 16-Bit fix-point numbers were used for the recorded ECG as well as for wavelet coefficients, scaling coefficients and threshold values. Considering the maximal values possibly appearing in the course of the WT, a multiplication of incoming data by 4 is possible. Therewith, the whole value range is involved and the inaccuracies introduced by rounding errors are reduced.

Simplicity of all employed operations: as mentioned before, the usage of the quadratic spline wavelet provides a low number of coefficients (namely 4 low-pass coefficients and 2 high-pass coefficients) thus fulfilling the first requirement on an effective real-time processing. Furthermore, the coefficients allow the calculation of the WT with only bit-shifts and additions. Also the adaptation of all threshold values was implemented by bit-



manipulations. All remaining steps of the algorithm are performed by logical instructions like comparisons. These operations also are characterized by their low computational load.

Avoidance of inappropriate processing methods: to provide a uniformly low computational load, often used undesirable steps as back-searches were excluded. The applied windowing operation, also an improper medium for the real-time purpose, acts on a window of 500 samples, introducing a delay of 250 ms only. All values to be updated in periodic manner (for example the zero crossings within  $W_0$ , for which the removal or addition of crossings is demanded due to the sliding window) are arranged in circular buffers. This allows the algorithm to work continuously on every incoming sample.

### 3 RESULTS

#### 3.1 Detection Performance

Table 1 yields the results of the performance evaluation accomplished under different conditions. Using the MIT-BIH Arrhythmia Database, all beats occurring beginning 5 minutes after the begin of the records until 30 minutes have been evaluated. This results in 90491 beats. As previously mentioned, the example trials *testing1* and *testing2* were carried out without any influence created by the usage of  $N_{cross}$ .

The quantitative evaluation of the complete method with own data (Table 1, *evalOwnData*) yielded a sensitivity (Se) of 99.85 % and a positive predictivity (+P) of 99.92 %. The annotation by a health professional was used as reference. The evaluation using the MIT-BIH Arrhythmia Database (Table 1, *evalMIT*) yielded a sensitivity and positive predictivity of 99.74 %, respectively 99.85 %. As the algorithm was designed for data sampled at 1000 Hz, the data was upsampled. Due to the contained frequency portions, the regularity analysis was skipped as a similarly easy regularity analysis (like accomplished for own data) no longer was possible.

Table 1: Performance of the QRS detector using different test configurations.

Identifier of the task	Number of beats	Se	+P
testing1	90941	99.31 %	99.80 %
testing2	90941	99.81 %	99.36 %
evalOwnData	8525	99.85 %	99.92 %
evalMIT	90941	99.74 %	99.85 %

Table 2: Required resources for signal processing.

Processing Step	Computational load (at 8 MHz)	
	<i>required cycles</i>	<i>required <math>\mu s</math></i>
Calculation of WT	900	112.5
Search for MMP	400	50
$N_{cross}$ maintenance	70	7.5
Over all	<2000	<250

Table 3: Memory coverage of the implemented method.

Code Memory	Data memory
<7900 byte	<4000 byte

#### 3.2 Computational Load

Table 2 contains an outline of the required resources. Besides the overall amount of cycles, the equivalent processing time and the number of cycles concerning specific steps within the implemented method are given. The algorithm acts without any prefiltering of the signal and thus avoids additional computations other than the calculation of the WT and the subsequent feature extraction procedure. The step “Search for MMP” refers to the search for extremas and the grouping of detected combinations of extrema to a MMP. According to the structure of the algorithm, this step is called twice per input sample, once for scale 4 and once for scale 5. The whole detection procedure requires less than 250  $\mu s$  (2000 cycles), leaving computing power to manage other functions.

Also of high interest considering the limited resources of the ultra-low power  $\mu C$  is the memory coverage. Table 3 shows the most important characteristics, proving the adequacy of the implemented method.

### 4 DISCUSSION

The evaluation of our method showed promising results in terms of the required computational load and the performance of the method. Note, that the only difference between the methods used in *testing1* and *evalMIT* is the correction of the threshold in scale 5, thus pointing out the effectiveness of the algorithm. Compared to the high-quality approaches of Li et al. (Li, 1995) and Martinez et al. (Martinez, 2004) the reached detection rates are slightly lower. However, a deeper

insight to the methods reveals in both cases strategies which are very impractical for a real-time calculation. For instance, Li et al. work on 600 samples of the ECG each time instead of on every incoming sample. Furthermore, two “real-time unfriendly” techniques (in the original paper referred to as “tactic 1” and “tactic 2”) to exclude or accept detections based on foregoing and subsequent detections with the benefit of hindsight were incorporated. In turn, Martinez et al. incorporated in the computation of their scale-dependent thresholds the RMS calculated from  $2^{16}$  values of the respective scale. The storage of that amount of data for one scale would exceed the data memory of the controller by a factor of 10. Taking this into account, our realization seems to be very appropriate for the application area. By incorporating the information on the latest detected QRS complexes, the performance of the method still can be slightly increased. Nevertheless, to reach the detection performance reported by Li et al. while maintaining a similarly low computational load like provided by our method seems to be very difficult.

In addition to the good results obtained by our method, the implemented method exhibits a high potential for future work. For instance, concerning the QRS delineation as well as P and T waves delineation, the already computed wavelet coefficients can be used as basis.

## 5 CONCLUSIONS

We developed a method especially suited to perform signal processing in close proximity to the sensor. The proposed algorithm is adapted to best meet the most important demands of the ambulatory application, which are low computational load and high reliability. Even for a sampling frequency of 1000 Hz the described method can be used on an ultra-low power  $\mu C$ , leaving computing power for other purposes. The physical proximity of the signal-processing hardware to the sensor provides increased flexibility for subsequent information handling and, combined with an ultra-low power architecture, is capable of significantly increasing the runtime of an ambulatory monitoring system.

Future work will focus on further signal processing steps. These steps may include detection of P and T-waves as well as the evaluation of the ST-segment. As it was shown by the literature this can be done based on the wavelet transform as well. The use of the wavelet coefficients for further signal processing purposes renders the wavelet-based method even more attractive for low-power microsystems with reduced hardware complexity.

## REFERENCES

- Dinh, H.; Kumar, D.; Pah, N. & Burton, P.: 'Wavelets for QRS detection', In Engineering in Medicine and Biology Society, 2001. Proceedings of the 23rd Annual International Conference of the IEEE, pp. 1883--1887.
- Goldberger AL, Amaral LAN, Glass L, Hausdorff JM, Ivanov PCh, Mark RG, Mietus JE, Moody GB, Peng CK, Stanley HE. *PhysioBank, PhysioToolkit, and PhysioNet: Components of a New Research Resource for Complex Physiologic Signals*. Circulation 101(23):e215-e220 [Circulation Electronic Pages; <http://circ.ahajournals.org/cgi/content/full/101/23/e215>]; 2000 (June 13).
- Holschneider, M.; Kronland-Martinez, R.; Morlet, J. Tchamitchian, P.: 'A Real-Time Algorithm for Signal Analysis with the Help of Wavelet Transform', Wavelets, Time-Frequency Methods and Phase Space, Springer Verlag, Berlin, 1989
- Li, C.; Zheng, C. & Tai, C., 1995, 'Detection of ECG characteristic points using wavelet transforms.', IEEE Trans Biomed Eng 42(1), 21-28.
- Köhler, B.; Hennig, C. & Orglmeister, R. *The principles of software QRS detection*. IEEE engineering in medicine and biology magazine : the quarterly magazine of the Engineering in Medicine & Biology Society., 2002, 21, 42-57
- Mallat, S. & Hwang, W. , 1992, 'Singularity detection and processing with wavelets', IEEE Transactions on Information Theory 38, 617-643.
- Martinez, J. P.; Almeida, R.; Olmos, S.; Rocha, A. P. & Laguna, P., 2004, 'A wavelet-based ECG delineator: evaluation on standard databases.', IEEE Trans Biomed Eng 51(4), 570-581.

## APPENDIX

Rules for threshold adaptation after a detected MMP (for lower thresholds  $\varepsilon_m^-$  “max” is replaced with the specific “min” values and  $\varepsilon_m^+$  is replaced by  $\varepsilon_m^-$ ):

```

if  $\max(X(2^m, i)) \geq 3 * \varepsilon_m^+$ 
     $\varepsilon_m^+ = 0.375 * \max(X(2^m, i)) + 0.625 * \varepsilon_m^+$ 
else if  $\max(X(2^m, i)) \geq 3 * \varepsilon_m^+$ 
     $\varepsilon_m^+ = 0.5 * \max(X(2^m, i)) + 0.5 * \varepsilon_m^+$ 
else if  $\max(X(2^m, i)) \geq 2 * \varepsilon_m^+$ 
     $\varepsilon_m^+ = 0.75 * \max(X(2^m, i)) + 0.25 * \varepsilon_m^+$ 
else
     $\varepsilon_m^+ = 1.125 * \max(X(2^m, i))$ 

```

400 ms after an adaptation (to avoid mistakes introduced by T waves with higher frequency portions) the threshold is lowered by 50%.